Research Article

Mou'ad A. Tarawneh*, Sherin Abdelkader Saraireh, Ruey Shan Chen*, Sahrim Hj Ahmad, Musab A. M. Al-Tarawni, Lih Jiun Yu, Bahia Othman Alsobhi, and David Hui

Mechanical reinforcement with enhanced electrical and heat conduction of epoxy resin by polyaniline and graphene nanoplatelets

Abstract: In this study, the effects of polyaniline (PANI) incorporation (3 wt% of PANI) and graphene nanoplatelets (GNPs) loading (0.1–0.7 wt%) on the mechanical, thermal, and electrical performance of epoxy matrix were investigated. The incorporation of 0.3 wt% GNPs optimally enhanced the bending strength, bending modulus, tensile strength, tensile modulus, and impact strength (90 MPa, 1422 MPa, 63 MPa, 602 MPa, and 8.29 kJm^{-2}, respectively). At 0.3 wt% GNPs, the hybridization effect optimally enhanced the glass transition behaviour of the epoxy nanocomposites. The electrical and thermal conductivities of epoxy were improved upon the inclusion of PANI, and this increase was further augmented when the GNPs content increased to 0.3 wt%. However, higher GNPs contents deteriorated the mechanical performance and electrical and heat conduction. Field emission scanning electron microscopy showed good filler distribution and effective interactions among the GNPs, PANI, and epoxy components with appropriate compositions.

Keywords: conducting polymer, nanocomposite, thermal properties

1 Introduction

Epoxy is a highly valuable thermoset used in a broad variety of applications such as coatings, adhesives, insulators in manufacturing, and as a matrix material in structural composites because of its low cost, good chemical resistance, high adhesive strength, and exceptional performance [1,2]. Nevertheless, cured epoxy easily breaks and cracks and has a minimal conductivity, which restricts its performance. Thus, the incorporation of relatively low percentages of nanoscale particles such as carbon-based fillers and conducting polymers is considered as a promising approach to develop multifunctional epoxy nanocomposites with excellent electrical properties and improved mechanical performance, which can broaden their field of applications in industry such as electronic devices and sensors [3,4].

Graphene nanoplatelets (GNPs) such as nanoscale carbon-based fillers have attracted a great attention because of excellent mechanical properties such as the high Young's modulus (0.5–1.0 TPa) [5], hardness (~110–120 GPa) [6], and fracture strength (125 GPa) [7], and high electrical (close to pure copper [6]) and thermal conductivities (~500 W/mK) [8,9]. Moreover, GNPs are believed to be perfect reinforcing components to alter the properties of polymers because of the large quantity of naturally existing graphite. The 2D quantum confinement of GNPs in the polymeric matrix and high surface area of GNPs makes them unique

* Corresponding author: Mou'ad A. Tarawneh, Department of Physics, College of Science, Al-Hussein Bin Talal University, P.O. Box 20, Ma'an, Jordan, e-mail: moaath20042002@yahoo.com
* Corresponding author: Ruey Shan Chen, Department of Applied Physics, Faculty of Science and Technology, Universiti Kebangsaan Malaysia, 43600, Bangi, Selangor, Malaysia, e-mail: chen@ukm.edu.my, tel: 6014-9388795
Sherin Abdelkader Saraireh: Department of Physics, College of Science, Al-Hussein Bin Talal University, P.O. Box 20, Ma'an, Jordan; Physics Department, Faculty of Sciences, Taibah University, Al-Madeina al-Munawarah, Saudi Arabia
Sahrim Hj Ahmad: Department of Applied Physics, Faculty of Science and Technology, Universiti Kebangsaan Malaysia, 43600, Bangi, Selangor, Malaysia
Musab A. M. Al-Tarawni: Center of Advanced Electronics and Communication Engineering, Faculty of Engineering and Environment, Universiti Kebangsaan Malaysia, 43600, Bangi, Selangor, Malaysia
Lih Jiun Yu: Department of Mechanical Engineering, Faculty of Engineering, Technology and Built Environment, UCSI University, No 1, Jalan Menara Gading, UCSI Heights (Taman Connaught), Cheras, 56000, Kuala Lumpur, Malaysia
Bahia Othman Alsobhi: Physics Department, Faculty of Sciences, Taibah University, Al-Madeina al-Munawarah, Saudi Arabia
David Hui: Department of Mechanical Engineering, University of New Orleans, New Orleans, LA 70148, United States of America

nanofillers, and in contrast to other carbon nanofillers, they show the enhanced capability in changing most properties [10,11].

Several works in the literature described the reinforcement effect of GNPs, typically on the thermal and electrical properties of epoxy nanocomposites. Based on the research work by Hashim and Jumahat on GNPs/epoxy composites, which were prepared using a combined solution compounding/high-shear milling technique, the inclusion of 0.3 wt% GNPs enhanced the critical stress intensity factor and tensile modulus by approximately 64 and 32%, respectively [12]. Atif et al. reported that the Young's modulus, tensile strength, fracture toughness, and Charpy impact toughness of nanocomposites filled with 0.3 wt% GNPs increased by 24, 31, 29, and 89%, respectively [13]. In another work, Prolongo et al. studied the effect of different types of GNPs with various thicknesses and lateral dimensions on the mechanical properties and thermal stability of epoxy matrix composites; the results revealed that nanocomposites incorporated with larger and thicker nanoplatelets exhibited lower glass transition temperatures and higher decomposition temperatures and moduli [14]. In addition, Imran and Shivakumar showed the increase in electrical conductivity by nine log cycles, double increment in thermal conductivity, and one-third increment in fracture toughness with the inclusion of 1 wt% GNPs into the epoxy matrix [15].

Polyaniline (PANI) is a conducting polymer in the electrically conducting polymer group and has been well examined because of its properties, such as the stability, simple production process, favourable environmental characteristics, distinctive protonic doping procedure, and low price [16,17]. The blending of epoxy with PANI is a useful process to improve the conductivity of thermosetting composites, and the structure of a continuous PANI network is greatly important in electrically conductive PANI/epoxy composites, as reported by many researchers [18,19]. Several PANI/epoxy composites have been produced for different applications, such as anticorrosion coatings and conducting paints. For example, PANI is a conductive filler material that can be incorporated into a matrix to enhance the anticorrosion effect with only a low loading of 1–3 wt% [20,21]. In a recent study of epoxy/PANI/graphene oxide (GO) hybrid composites, the tensile strength and Young's modulus of the PANI/GO hybrid filler at 3 wt% in the epoxy nanocomposites were improved by 14.3 and 33.1%, respectively, compared to neat epoxy [22].

In recent years, the research on thermosetting composites that applied a conducting filler and a secondary filler has received much attention from researchers. For instance, Amin et al. prepared epoxy/PANI/multi-walled

carbon nanotubes (MWCNTs) nanocomposites in the form of microtubules with a relatively high aspect ratio via in situ oxidative polymerization, and the finding showed that the interconnection among the PANI/nanoparticles at low amount could form obvious conducting pathways and great interaction between PANI/MWCNTs and the epoxy matrix [23]. Wang et al. synthesized the insulated PANI coated CNT (rPANI@CNT)-reduced graphene oxide (rGO) hybrids with different loadings of rPANI@CNT that were introduced into epoxy resin; the researchers found that the dielectric constant at 100 Hz of the rPANI@CNT-rGO (ratio 1:1) epoxy resin composite with 0.75 wt% rPANI@CNT was 210 [24]. Lin et al. reported that the mechanical results showed the increase in initial modulus and ultimate tensile strength for the epoxy composite filled with 0.5 wt% poly(styrenesulfonate) (PSS)-PANI/rGO by approximately 22 and 51%, respectively [25]. Although the inclusion of organic components or inorganic fillers inside the polymer matrix has been proven to improve electrical and dielectric properties, it could destroy the mechanical properties. Thus, a synergistic balance between mechanical and electrical properties can be obtained using combinations of conductive polymers with carbon-based fillers in polymeric matrix composites to improve the charge transfer ability. Polymer nanocomposites with a low loading of conducting filler were reported to achieve excellent conductivity without decreasing the mechanical properties [26].

Numerous works have focused on the synthesis of epoxy nanocomposites reinforced with PANI/rGO through in situ oxidative polymerization and chemical modification of fillers [23,24]. However, the hybridization of PANI/GNPs in developing a conductive epoxy nanocomposite with balanced electrical conductivity and mechanical properties using a simple and direct melt-blending method to achieve high extent of GNP dispersion in epoxy resin at very little nanofiller loading remains limited. In this work, the blending of epoxy with various loadings of GNPs (0.1–0.7 wt%) and a constant amount of PANI (3 wt%) was carried out using a mechanical mixer assisted by the ultrasonication of hybrid fillers, and the mechanical, thermal, and electrical conductivity properties of the samples were studied.

2 Experimental details

2.1 Materials

Epoxy resin comprises a group of bisphenol A and epichlorohydrin with an equivalent weight of 184–190 and a

density of 1.16 kg/L, and polyetheramine D-230 as a hardener was supplied from Asachem (Malaysia) Sdn. Bhd. Needle-like PANI black green powder (purity: >99 wt%, yield: 40 wt%, conductivity: 4 W/cm^2; average diameter: 8 μm; length: 100 Å; and electrical conductivity: 2.7 S/cm) was supplied by E-TEK Co. Ltd., Korea. The GNPs (purity: >99.5 wt%; diameter: 5–10 nm; thickness: 4–20 nm; density: 0.23 g/cm^3, layers: <30; volume resistivity: 4 × 10^{-4} ohm cm) were supplied by Chengdu Organic Chemicals Co., Ltd. Chinese Academy of Sciences.

Table 1: Epoxy with various compositions of PANI and GNPs loadings

Sample code	Epoxy (wt%)	PANI (wt%)	GNPs (wt%)
Epoxy	100.0	0	0
Epoxy/PANI	97.0	3	0
Nanocomposites (NC1)	96.9	3	0.1
Nanocomposites (NC2)	96.7	3	0.3
Nanocomposites (NC3)	96.5	3	0.5
Nanocomposites (NC4)	96.3	3	0.7

2.2 Sample preparation

Six samples with different formulation were prepared as described in Table 1. The schematic diagram of the preparation of epoxy, epoxy/PANI, and epoxy/PANI/GNPs nanocomposites is presented in Figure 1. For the three-component system, the 3 wt% PANI powders were first mixed with different loadings of GNPs; then, the PANI/GNPs mixture was mixed with epoxy with a mechanical stirring machine for 1 h at 750 rpm. To avoid the formation of aggregates, the mixtures were sonicated using a probe sonicator (Model: Hielscher UP400S, 400 watts, 24 kHz) for 3 h. During sonication, the mixture container was held in an ice bath to avoid overheating the suspension so that the temperature was maintained at 40°C. After sonication, the hardener (polyethylene D230) was added into the mixture at a ratio of 3:1, and the mixture was gently stirred for 5 min. Then, the mixture was pumped under vacuum for 10 min to eliminate any trapped air. In the final stage, all samples were cured for 24 h at room temperature and subsequently post-cured for 2 h at 80°C and 1 h at 110°C to stabilize and remove air bubbles.

2.3 Characterization

A bending test was performed with a three-point flexural test machine (Testometric M350-10CT model) based on
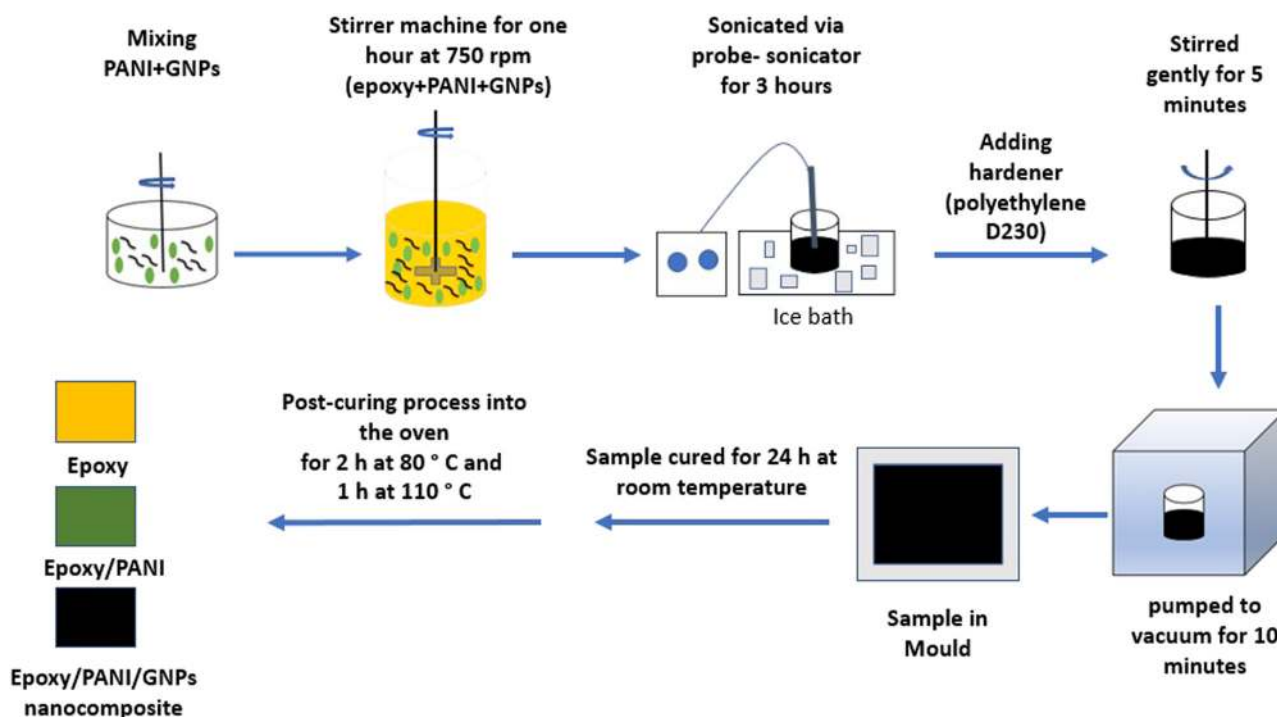

Figure 1: Schematic diagram of the epoxy/PANI/GNPs melt-blending process.

the ASTM D790 standard, a load cell of 1,000 N and a cross-head speed of 1.37 mm/min. The dimensions of the specimens in this study were $127.0 \times 12.7 \times 3.0$ mm^3. The values were taken from an average of six samples.

The Izod impact strength test was performed at a load weight of 0.898 kg and a velocity of 3.45 m/s using a Ray–Ran Pendulum Impact System in accordance with ASTM D 256-90b. The sample dimensions were $63.0 \times 12.7 \times 3.0$ mm^3. The average value from six replicates was reported for each composition.

Differential scanning calorimetry (DSC) and thermogravimetric analysis (TGA) were run using a Mettler Toledo DSC 882^e and a TGA/SDTA851^e, respectively, with 15–20 mg of samples. The DSC samples were heated from 30 to 200°C at a rate of 10°C/min and subsequently cooled at the same rate under atmospheric air flow condition. The samples for TGA were tested from 30 to 600°C at a heating rate of 10°C/min.

The electrical conductivity of the samples was measured using a high-frequency response analyser (HFRA Solartron 1256; Schlumberger) from 0.1 Hz to 1 MHz. The sample was inserted between two stainless steel electrodes with a surface contact area of 2 cm^2 and subsequently mounted onto the holder. The bulk resistance (R_b (Ω)) of the samples was determined from the obtained Cole–Cole plots using Z-View software. The conductivity was determined according to equation (1):

$$\sigma = L/R_b \cdot A, \tag{1}$$

where L denotes the thickness of the sample (cm), and A denotes the effective contact area (cm^2) of the electrode and electrolyte.

The thermal conductivities of the samples (one specimen was tested per composite type) were measured using a thermal conductivity analyser (TCA, Nanoflash NETZSCH, model LFA 44712-41). Disc-type samples (with a diameter of 12.7 mm and a thickness of 1 mm) were put in an electric furnace. The thermal conductivity (λ, W m^{-1} K^{-1}) of the samples, which depends on the thermal diffusivity (α, mm^2 s^{-1}), density (ρ, g cm^{-3}), and specific heat capacity (C_p, J g^{-1} K^{-1}), was calculated at various temperatures from 30 to 180°C by the following equations:

$$\lambda(T) = \alpha(T) \cdot \rho(T) \cdot C_p(T), \tag{2}$$

$$\alpha = 0.1388 \times \frac{d^2}{t_{1/2}}, \tag{3}$$

$$C_p = \frac{Q}{m \cdot \Delta t}, \tag{4}$$

where d is the sample thickness (mm), $t_{1/2}$ is the time when T/T_{max} reaches 0.5, m is the sample mass, Q is the energy absorbed by the sample, and T_{max} is the maximum rear-side temperature increase. To calculate the heat capacity, pyroceram with the thickness of 12.7 mm was used as reference specimen.

The morphology of the samples was examined using high-resolution field emission scanning electron microscopy (FESEM, model SUPRA 55VP). The fracture surfaces of the impact test specimens were sputter coated with platinum before being studied by FESEM to avoid the charging effect and obtain a clear image.

3 Results and discussion

3.1 Mechanical properties

The bending, tensile, and impact properties of neat epoxy, epoxy/PANI, and GNPs nanocomposites with different filler loadings are presented in Figure 2. In comparison to neat epoxy, the failure of the mechanical properties induced by the PANI component is primarily because of two causes. First, PANI acts as a non-reinforcing filler because of important differences in the crystallinity and polarity from the epoxy polymer; second, micro-voids and clusters form because of the enhanced viscosity of the composite [27].

The incorporation of GNPs significantly affected the flexural and tensile properties of nanocomposites, as indicated in Figure 2. The bending strength and bending modulus of pure epoxy improved with a 0.3 wt% loading of GNPs (NC2 nanocomposites) but subsequently gradually decreased with higher contents of GNPs. Compared to pure epoxy, the presented improvements in both bending strength and modulus of the NC2 nanocomposites were 14 and 25%, respectively. These improvements can be ascribed to the strong reinforcement effects of graphene, appropriate compatibility, and excellent interactions of the filler/epoxy matrix interface, which results in an efficient load distribution from the matrix to the filler [1]. However, with an additional increase in GNPs loadings, the bending properties of NC3 (0.5 wt%) and NC4 nanocomposites (0.7 wt%) deteriorated. This result is in agreement with previous studies on GO/epoxy by Chhetri et al. [28] and GNPs/epoxy composites by Shen et al. [29], which showed the optimal enhancement in flexural properties at 0.1 and 0.25 wt%, respectively.

As shown in Figure 2, the tensile properties revealed a trend similar to the flexural properties. Compared to pure epoxy, the tensile strength and modulus of the
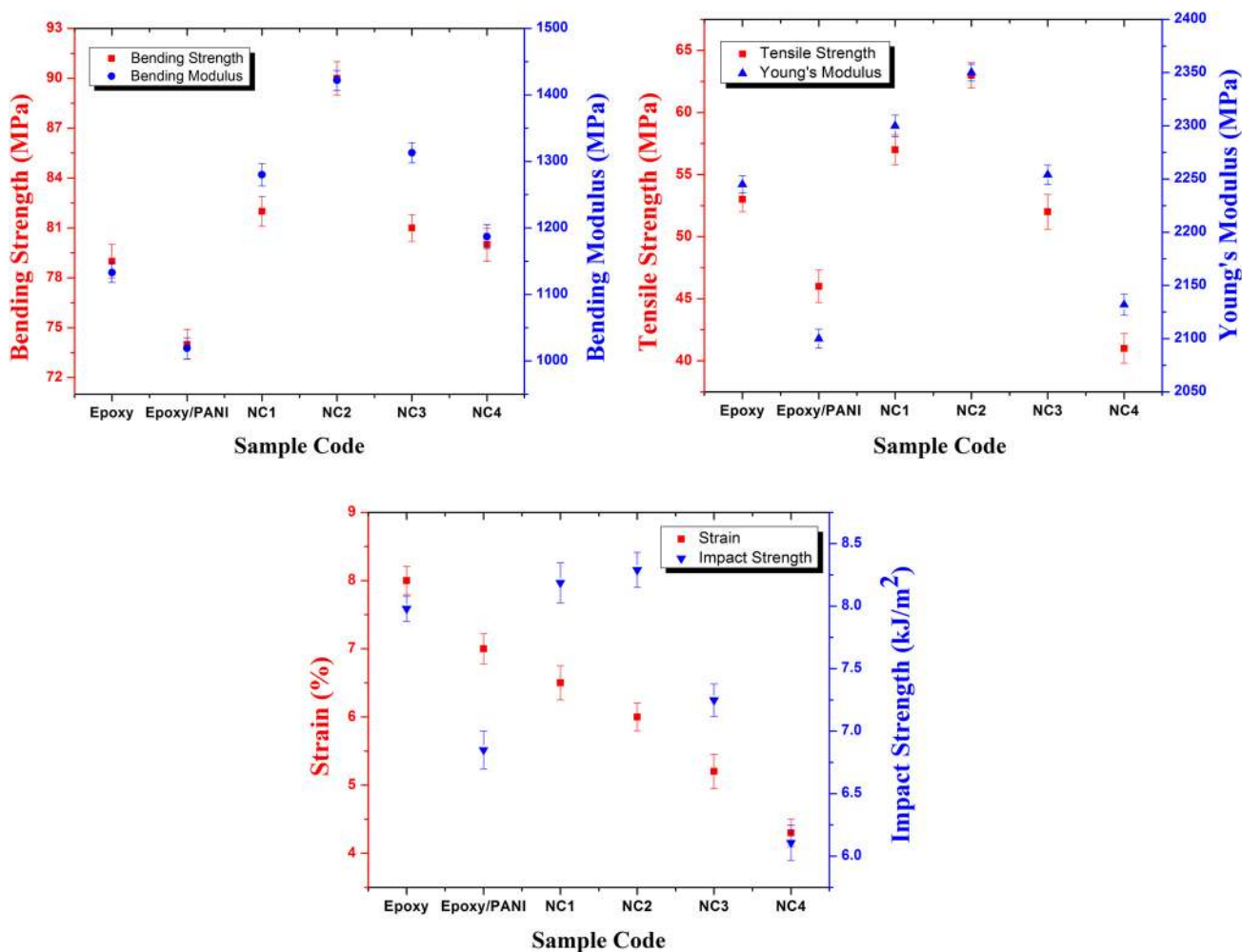
Figure 2: Mechanical properties of epoxy, epoxy/PANI, and epoxy/PANI/GNPs nanocomposites.

NC2 nanocomposite increased by 19 and 5%, respectively. These remarkable increases may be because GNPs as physical crosslinking areas limit the movement of the epoxy chains under a load. Similarly, the increase in tensile strength and Young's modulus of epoxy by 23 and 10% were reported at 0.25 and 0.5 wt% GNPs, respectively, as reported by Shokrieh *et al.* [30]. Beyond the addition of 0.3 wt% GNPs, the tensile properties deteriorated with increasing GNPs loading. The reason is the nonuniform dispersion and agglomeration of GNPs/PANI at higher contents inside the epoxy matrix, where the packing behaviour of graphene arises from the high aspect ratio and van der Waals forces of GNPs. These agglomerates act as stress concentrators with the weakest areas at the centre points, which reduces the properties of the nanocomposites as described by Pour *et al.* who reported the lower mechanical strengths when the GO levels were more than 0.5 wt% in epoxy [31].

The strain of epoxy/PANI and NC1, NC2, NC3, and NC4 nanocomposites showed a continuous and significant reduction in Figure 2. This result can be ascribed to the increased rigidity of the epoxy matrix. The inserted GNPs/PANI fillers in the epoxy acted as limitation points for the polymer chain movement, which made the nanocomposites more brittle [32]. Nevertheless, the impact strength in Figure 2 displays the maximum enhancement in the NC2 nanocomposite because the homogeneous dispersion was restricted up to a GNPs concentration of 0.3 wt%. However, at higher GNPs loadings in NC3 and NC4, the significantly decreased impact strength might be because of the fillers agglomeration, which can produce unexpected internal deficiencies such as cracks to result in weaknesses and smaller energy absorption in the epoxy nanocomposite. The toughness enhancement is believed to depend on the stress concentration factor that is related to the size of graphene; for instance, 0.1 wt%

GO was optimally obtained in epoxy [33], and 1.5 wt% [34] and 3 wt% GNPs [35] were achieved in TPNR.

3.2 DSC analysis

In this work, DSC was performed to test the thermal properties including measuring the glass transition temperature (T_g). T_g denotes the temperature range in which the thermoset polymer changes from hard, rigid, or "glass"-like to more flexible, submersible, or "elastic". Based on Figures 3 and 4, the T_g of neat epoxy is located at 53.7°C, and the T_g of epoxy/PANI is at 53.4°C. Moreover, the analysis showed that the T_g shifted to higher values with the inclusion of GNPs/PANI in the epoxy matrix. The T_g of the nanocomposites increased by 1.1 and 3.3°C when the GNP content was 0.1 and 0.3 wt%, respectively. Increasing the weight percentage of GNPs from 0.5 to 0.7 wt% showed that the T_g decreased to 54.76 and 54.58°C, respectively, compared to nanocomposites containing 0.3 wt% GNPs. This trend occurs because the GNPs and PANI acted as physical interlocking points in the epoxy matrix, which limited the movement of epoxy chains. Moreover, the reduction in T_g might be caused by the decrease in crosslinking density or the extent of curing in the epoxy matrix. The increasing content of GNPs can induce the formation of aggregates that create physical defects, which obstructs the crosslinking of the epoxy matrix with the hardener and decreases the crosslinking density. For instance, Lin *et al.* found that the addition of PSS-PANI/rGO up to 1 wt% decreased the
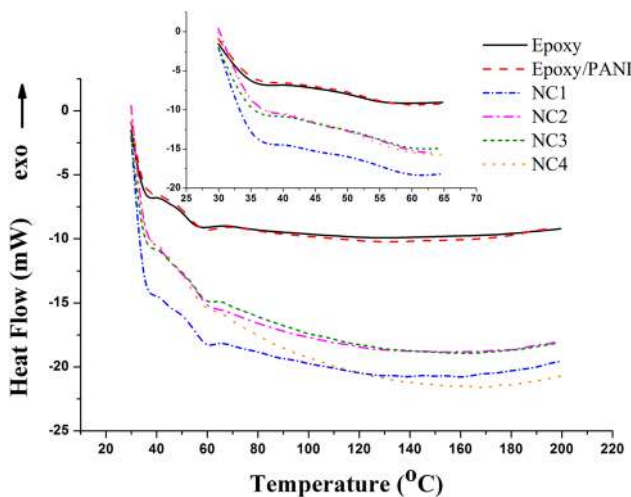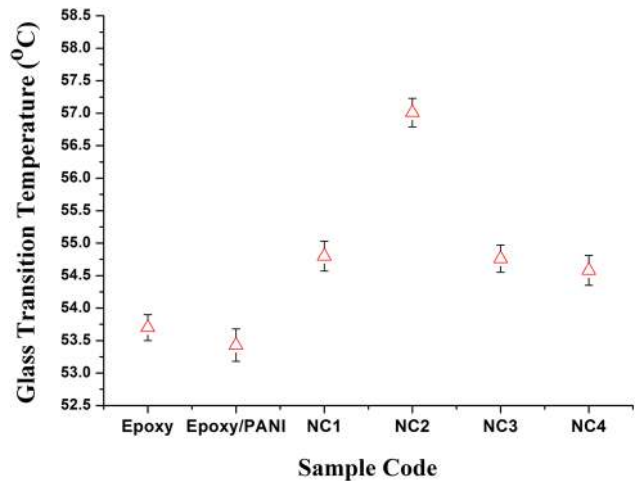
Figure 4: Glass transition temperature of epoxy, epoxy/PANI, and epoxy/PANI/GNPs nanocomposites.

crosslinking density of epoxy matrix because of the filler agglomeration [25]. The development of aggregates also provides free volume at the interface, which increases the mobility of the segments. The decline in T_g of NC3 and NC4, as shown in Figures 3 and 4, could be caused by the restacking of GNPs sheets and PANI, which also form clusters in the matrix.

3.3 Thermogravimetric analysis

Figure 5 displays the TGA and DTG curves to study the thermal stability of epoxy, epoxy/PANI, and epoxy/PANI/GNPs nanocomposite samples. The TGA data for all studied samples are described in Table 2. All investigated samples show a comparable thermal behaviour to DSC. Figure 5 shows that all samples exhibited a one-step decomposition process. For pure epoxy, the early decomposition began at a $T_{10\%}$ of 336.9°C and initially ended (which was recorded at a weight loss of 90%) at 445.4°C. By adding PANI into epoxy, the decomposition process was accelerated, as presented in the inset image in Figure 5, and the curves shifted to the left side. Moreover, the decomposition temperatures were lower ($T_{10\%}$ = 316.2°C) for the epoxy/PANI composite than those of the pure epoxy (Table 2). This result can be correlated with the initial decomposition of PANI at 153–295°C [36], where the same range of temperature for the pure PANI has been reported by Saritha and Sunil [37]. When GNPs were incorporated into epoxy/PANI, the rate of decomposition changed with the GNP loading. At a lower GNP loading (0.1 wt%) in NC1, the curve shifted to the left, and $T_{10\%}$ decreased to 306.2°C; however, the 90%
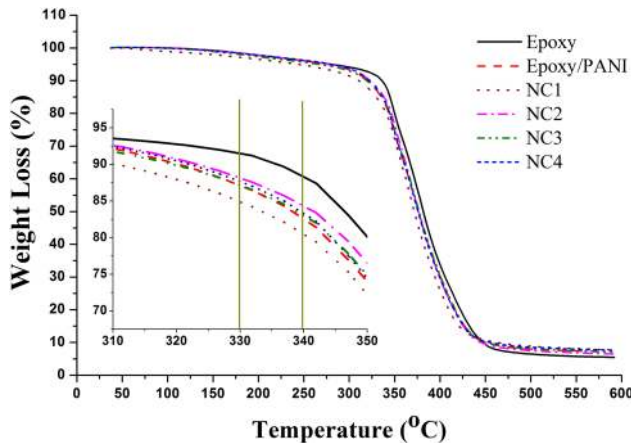
Figure 3: DSC thermograms of epoxy, epoxy/PANI, and epoxy/PANI/GNPs nanocomposites.

Figure 5: TGA thermograms of epoxy, epoxy/PANI, and epoxy/PANI/GNPs nanocomposites.

Table 2: TGA data of epoxy, epoxy/PANI, and epoxy/PANI/GNPs nanocomposites

Sample (ID)	$T_{10\%}$ (°C)	$T_{90\%}$ (°C)	Total decomposition mass (%)	Residual mass (%)
Epoxy	336.9	445.4	94.75	5.42
Epoxy/PANI	316.2	449.0	92.87	7.29
NC1	306.2	462.5	92.45	7.67
NC2	321.1	446.3	93.77	6.43
NC3	318.6	450.2	93.17	7.01
NC4	321.8	453.5	92.56	7.60

Note: $T_{10\%}$ denotes the temperature where the decomposition showed 10% weight loss, and $T_{90\%}$ denotes the temperature where the decomposition shows 90% weight loss.

decomposition point occurred at 462.5°C possibly may be because the nanofiller loading was too low and insufficient to cause a good distribution of GNPs. Interestingly, the TGA curves shifted back to higher temperatures with higher loadings of GNPs. At 0.3–0.7 wt% GNPs, the decomposition process was delayed (compared to that of epoxy/PANI), where $T_{10\%}$ were recorded at 321.1, 318.6, and 321.8°C, respectively, although they were still lower than that of pure epoxy. Thus, a higher thermal resistance occurred, which is a consequence of the effective interaction between GNPs and the epoxy because of the good dispersion and distribution of GNPs. In addition, the improved thermal stability can be correlated with the creation of a carbonaceous char structure during thermal oxidation [38].

The residue contents left after the decomposition process at 450°C are displayed in Table 2. The least amount of residual mass was found in pure epoxy

(5.42%). Remarkably, when the GNPs and PANI were incorporated, the increase in residue amounts was 6.43–7.76%. The increased content of residue is ascribed to the existence of the PANI/GNPs, which is retained even after the decomposition of epoxy, which is consistent with the results of Rahnamol and Gopalakrishnan (2020) who incorporated 3 wt% PANI/GO hybrid in epoxy resin [22]. Moreover, GNPs can alter the thermal degradation path at high temperatures and endorse the formation of char from epoxy, as described in the previous study on epoxy/graphene nanosheets [39].

3.4 Electrical conductivity

The electrical conductivity of epoxy/PANI nanocomposites with various loadings of GNPs is presented in Table 3. Neat epoxy exhibited an electrical conductivity of 7.83×10^{-8} S/m, which implies an insulating behaviour; this result is consistent with the literature [40]. For the epoxy/PANI composite, the conductivity improved to 6.05×10^{-7} S/m at a 3 wt% loading. By adding GNPs, the conductivity of the NC1 (0.1 wt% GNPs) nanocomposite increased to 7.39×10^{-5} S/m, and the NC2 (0.3 wt% GNPs) nanocomposites showed a slightly higher conductivity of 8.72×10^{-5} S/m. This could be related to the better GNPs dispersion and interaction linkage of GNPs with epoxy/PANI as observed in Figure 8(d). In this condition, an effective conductive path can be created via GNPs layers with the PANI components to link the gap between GNPs layers and form a suitable percolating network structure in the matrix, which enables the electrons to pass through direct "contacts" between the conductive fillers [41–43], as illustrated in Figure 6. However, at higher loadings of GNPs, the electrical conductivity has poor performance. The epoxy nanocomposites with 0.5 wt% GNPs (NC3) and 0.7 wt% GNPs (NC4) had electrical conductivities of 2.44×10^{-5} and 8.09×10^{-6} S/m, respectively. This is possibly because the decreased

Table 3: Electrical conductivity of epoxy, epoxy/PANI, and epoxy/PANI/GNPs nanocomposites

Sample code	Electrical conductivity, σ (S/m)
Epoxy	7.83×10^{-8}
Epoxy/PANI	6.05×10^{-7}
NC1	7.39×10^{-5}
NC2	8.72×10^{-5}
NC3	2.44×10^{-5}
NC4	8.09×10^{-6}
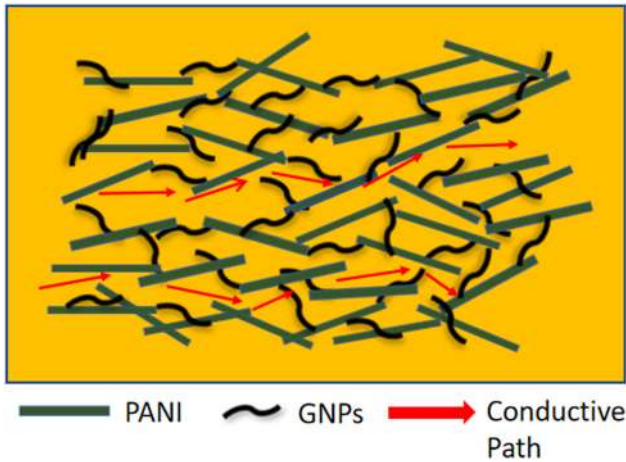
Figure 6: Schematic diagram of the conductive path inside the epoxy/PANI/GNPs (NC2) nanocomposites.

Figure 7: Thermal conductivity of epoxy, epoxy/PANI, and epoxy/ PANI/GNPs nanocomposites.

interaction of the GNPs and PANI, which is caused by their random agglomeration along with a small aspect ratio of unity, makes it difficult in forming conductive networks in the insulating epoxy matrix [44].

3.5 Thermal conductivity

The thermal conductivity of epoxy, epoxy/PANI, and NC samples is displayed in Figure 7. The thermal conductivity of all samples increased with increasing temperature from 30 to 120°C. Furthermore, the effect of temperature on the thermal conductivity was insignificant when the testing temperature exceeded 120°C. NC2 had higher thermal conductivity than neat epoxy and the other samples at all measured temperatures. For instance, the increased thermal conductivity of NC2 at 30, 60, 90, and 120°C records for approximately 30, 31.3, 35.3, and 39%, respectively, compared to the pure epoxy. This improvement in thermal conductivity might be because the intrinsic thermal conductivity of the GNPs and PANI is much higher than that of pure epoxy [44]. Another possible reason for the increase in thermal conductivity is the homogeneous dispersion of GNPs/PANI fillers in the epoxy matrix which led to the increased interfacial area and the reduced interfacial thermal resistance of epoxy and GNPs/PANI. Yu *et al.* [45,46] noted that the low interfacial thermal resistance contributed by GNPs is ascribed to the decreased geometric contribution of phonon scattering at the interfaces. Furthermore, the GNPs/PANI components act as a phonon transport bridge and enable for the complete heat transfer within the epoxy nanocomposite. As observed in Figure 7, the thermal
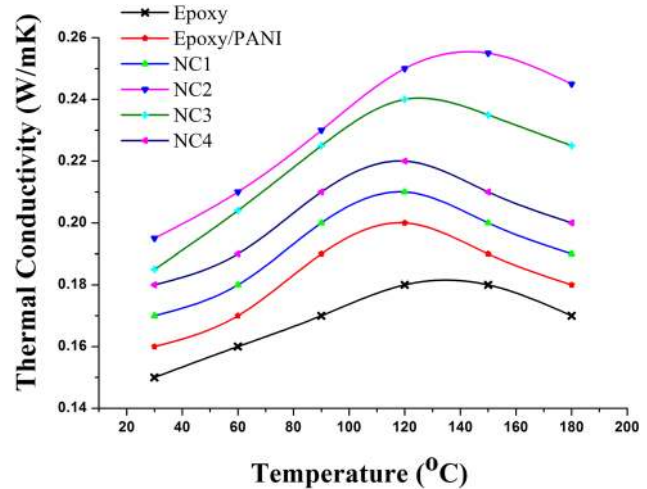
conductivity began to decrease with NC3 and NC4 because of the presence of agglomerated clusters and voids as strong thermal barriers, which significantly decrease the thermal conductivity of the nanocomposites [47–49].

3.6 Morphological analysis

To examine the dispersion of hybrid PANI/GNPs in the epoxy matrix, the impact fractured surfaces of pure epoxy, epoxy/PANI, and GNPs filled nanocomposites were analysed. As displayed in Figure 8a, the surface of pure epoxy is smooth with various river patterns because of the extremely brittle type of epoxy. However, Figure 8b shows a relatively rough fractured surface of the epoxy/3 wt% PANI samples with holes, which appear to have a beehive shape. As shown in Figure 8c and d, the GNPs/PANI fillers were uniformly dispersed in the epoxy matrix without showing much agglomeration in the NC1 and NC2 samples. Especially in NC2 nanocomposite, Figure 8d displays a less extreme variation in the microstructure where the smooth/ rough phase and distribution of holes are approximately identical in the micrograph. At low magnification, the image of the NC2 nanocomposites in Figure 8d shows the embedment of platelets in the holes or gaps of matrix and this confirms the presence of appropriate interactions and the good compatibility among the GNPs, PANI, and epoxy matrix. In addition, no obvious clusters of filler can be found, and the interactions seem to provide a network-like structure. This observation supports the significant improvement in the properties of the nanocomposites than that of pure epoxy. In the case of NC3 and NC4, as
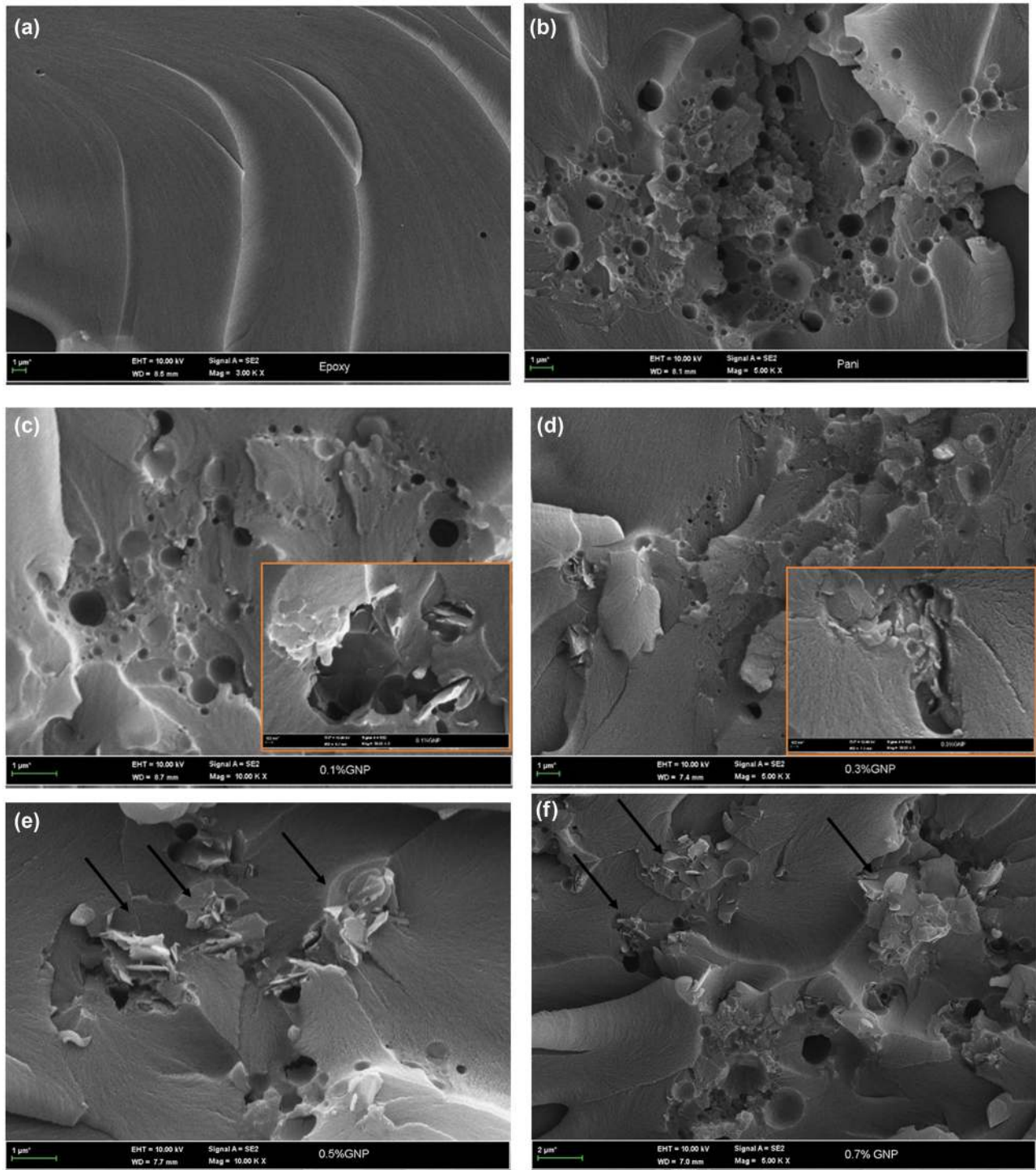
Figure 8: FESEM micrographs of (a) epoxy, (b) epoxy/PANI, (c) NC1, (d) NC2, (e) NC3, and (f) NC4.

indicated in Figure 8e and f, many agglomerations of GNPs/PANI on the epoxy matrix surface are obvious, and the layered structure of GNPs is clearly visible in the NC3 and NC4 nanocomposites, as indicated by the black arrows. The agglomerates normally delaminate through the fracture process because of the weak adhesion between the

fillers and the matrix. These agglomerates have an adverse effect on improving the performance of nanocomposites.

According to the FESEM micrographs in Figure 8, a schematic model of the epoxy, epoxy/PANI, and epoxy/PANI/GNPs nanocomposites is presented in Figure 9. As a control sample, the epoxy system that acts as the
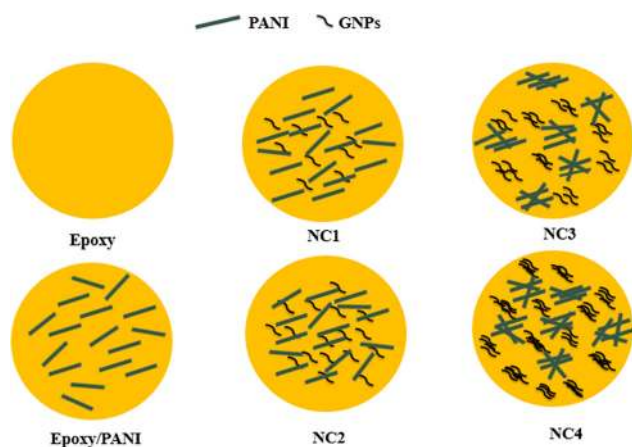
Figure 9: Schematic diagram of epoxy, epoxy/PANI, and epoxy/GNPs/PANI nanocomposites.

polymeric matrix is represented by a smooth and one-phase surface. With the inclusion of 3 wt% PANI into the epoxy matrix, the added PANI with a needle-like dimension [50] (as represented by the rectangular shape) is expected to distribute well in the composite. The small amount of GNPs corresponds to an insufficient GNPs–PANI interaction in NC1 where the smooth and rough surfaces were obviously visible in different spot as shown in Figure 8c. In comparison, the distribution and dispersion of the GNPs (flaky GNP is presented by a crooked line) and PANI in the NC2 nanocomposite (which is consistent with Figure 8d) system show good polymer–filler contact because of the π–π interactions and hydrophobic–hydrophobic interactions [49,51], which effectively reinforces impact in the system, as previously highlighted. When the GNPs content is higher, such as in the NC3 and NC4 systems, the GNPs and PANI components experience intracellular localization, which promotes the formation of agglomerates in more clusters. For example, an inhomogeneous dispersion of GNPs is produced because of the increasing amount of GNPs in the system and increasing size of the PANI cluster.

4 Conclusions

Epoxy composites filled with both PANI and GNPs were successfully prepared at different GNP loading levels and systematically investigated. The bending strength, bending modulus, tensile strength, and tensile modulus of the NC2 nanocomposites containing 0.3 wt% GNPs were improved by 14, 25, 19, and 8%, respectively, in comparison to those of neat epoxy. Moreover, with the incorporation of fillers in

NC2, the T_g of the composites was improved by 3.3°C. The presence of GNPs changed the thermal degradation path of epoxy and endorsed the formation of char, where the char residues from the epoxy nanocomposite increased with the GNPs content. The analysis of the complex impedance method revealed that the electrical conductivity was significantly enhanced from 7.83×10^{-8} to 8.72×10^{-5} S/m for NC2, which was significantly higher than those with higher GNPs contents (NC3 and NC4). Furthermore, the GNPs/PANI fillers increased the thermal conductivity of the nanocomposites by 30–39% at a low filler loading of only 0.3 wt% GNPs in the epoxy systems. In summary, the incorporation of PANI/GNPs in the epoxy composite enhanced the mechanical and conductivity properties of the composite. This finding will provide a source for the structural applications of conductive composites.

Conflict of interest: The authors declare no conflict of interest regarding the publication of this paper.

References

[1] Qi B, Lu S, Xiao X, Pan L, Tan F, Yu J. Enhanced thermal and mechanical properties of epoxy composites by mixing thermotropic liquid crystalline epoxy grafted graphene oxide. Express Polym Lett. 2014;8(7):467–79.

[2] Wei J, Vo T, Inam F. Epoxy/graphene nanocomposites – processing and properties: a review. RSC Adv. 2015;5(90):73510–24.

[3] Gu H, Ma C, Gu J, Guo J, Yan X, Huang J, et al. An overview of multifunctional epoxy nanocomposites. J Mater Chem C. 2016;4(25):5890–906.

[4] Roy S, Petrova RS, Mitra S. Effect of carbon nanotube (CNT) functionalization in epoxy-CNT composites. Nanotechnol Rev. 2018;7(6):475–85.

[5] Chen RS, Amran NAM, Ahmad S. Reinforcement effect of nanocomposites with single/hybrid graphene nanoplatelets and magnesium hydroxide. J Therm Anal Calorim. 2019;137(1):79–92.

[6] Konakov V, Kurapova OY, Solovyeva E, Lomakin I, Archakov IY. Synthesis, structure and mechanical properties of bulk "copper-graphene" composites. Rev Adv Mater Sci. 2018;57(2):151–7.

[7] Wu Y, Tang B, Liu K, Zeng X, Lu J, Zhang T, et al. Enhanced flexural properties of aramid fiber/epoxy composites by graphene oxide. Nanotechnol Rev. 2019;8(1):484–92.

[8] Ghouri ZK, Motlak M, Afaq S, Barakat NAM, Abdala A. Template-free synthesis of Se-nanorods-rGO nanocomposite

for application in supercapacitors. Nanotechnol Rev. 2019;8(1):661–70.

[9] Glukharev AG, Konakov VG. Synthesis and properties of zirconia–graphene composite ceramics: a brief review. Rev Adv Mater Sci. 2018;56(1):124–38.

[10] Ahmed AK, Atiqullah M, Al-Harthi MA, Abdelaal AF, Pradhan DR. Non-isothermal crystallization of Ziegler Natta i-PP-graphene nanocomposite: DSC and new model prediction. Can J Chem Eng. 2020;98(6):1398–410.

[11] Liang J, Du Q. Melt flow and flexural properties of polypropylene composites reinforced with graphene nano-platelets. Int Polym Proc. 2018;33(1):35–41.

[12] Hashim UR, Jumahat A. Improved tensile and fracture toughness properties of graphene nanoplatelets filled epoxy polymer via solvent compounding shear milling method. Mater Res Express. 2018;6(2):025303.

[13] Atif R, Shyha I, Inam F. The degradation of mechanical properties due to stress concentration caused by retained acetone in epoxy nanocomposites. RSC Adv. 2016;6(41):34188–97.

[14] Prolongo SG, Jimenez-Suarez A, Moriche R, Urena A. Graphene nanoplatelets thickness and lateral size influence on the morphology and behavior of epoxy composites. Eur Polym J. 2014;53:292–301.

[15] Imran KA, Shivakumar KN. Enhancement of electrical conductivity of epoxy using graphene and determination of their thermo-mechanical properties. J Reinf Plast Compos. 2018;37(2):118–33.

[16] Borsoi C, Zattera A, Ferreira C. Effect of cellulose nanowhiskers functionalization with polyaniline for epoxy coatings. Appl Surf Sci. 2016;364:124–32.

[17] Gao XZ, Liu HJ, Cheng F, Chen Y. Thermoresponsive polyaniline nanoparticles: preparation, characterization, and their potential application in waterborne anticorrosion coatings. Chem Eng J. 2016;283:682–91.

[18] Bhadra J, Alkareem A, Al-Thani N. A review of advances in the preparation and application of polyaniline based thermoset blends and composites. J Polym Res. 2020;27(5):122–42.

[19] Perrin F, Oueiny C. Polyaniline thermoset blends and composites. React Funct Polym. 2017;114:86–103.

[20] Sakhri A, Perrin F, Aragon E, Lamouric S, Benaboura A. Chlorinated rubber paints for corrosion prevention of mild steel: a comparison between zinc phosphate and polyaniline pigments. Corros Sci. 2010;52(3):901–9.

[21] Sathiyanarayanan S, Muthukrishnan S, Venkatachari G. Effects of polyaniline content in chlorrub-based coatings on corrosion protection of steel. J Appl Polym Sci. 2006;102(4):3994–9.

[22] Rahnamol A, Gopalakrishnan J. Improved dielectric and dynamic mechanical properties of epoxy/polyaniline nanorod/ *in situ* reduced graphene oxide hybrid nanocomposites. Polym Compos. 2020;41(8):1–16.

[23] Imani A, Arabi M, Farzi G. Effect of in-situ oxidative preparation on electrical properties of Epoxy/PANi/MWCNTs nanocomposites. J Mater Sci Mater Electron. 2016;27(10):10364–70.

[24] Wang T, Yuan L, Liang G, Gu A. Polyaniline coated carbon nanotube/graphene "sandwich" hybrid and its high-k epoxy composites with low dielectric loss and percolation threshold. Appl Surf Sci. 2015;359:754–65.

[25] Lin YT, Don TM, Wong CJ, Meng FC, Lin YJ, Lee SY, et al. Improvement of mechanical properties and anticorrosion performance of epoxy coatings by the introduction of polyaniline/graphene composite. Surf Coat Technol. 2019;374:1128–38.

[26] Harito C, Bavykin DV, Yuliarto B, Dipojono HK, Walsh FC. Polymer nanocomposites having a high filler content: synthesis, structures, properties, and applications. Nanoscale. 2019;11(11):4653–82.

[27] Khandelwal V, Sahoo SK, Manik G, Biswas K. Carbon nanotubes and polyaniline filled hybrid epoxy composites: assessing the viscoelastic behavior and mechanical properties. Polym Compos. 2019;40(S2):E1143–50.

[28] Chhetri S, Adak NC, Samanta P, Mallisetty PK, Murmu NC, Kuila T. Interface engineering for the improvement of mechanical and thermal properties of covalent functionalized graphene/epoxy composites. J Appl Polym Sci. 2018;135(15):46124.

[29] Shen MY, Chang TY, Hsieh TH, Li YL, Chiang CL, Yang H, et al. Mechanical properties and tensile fatigue of graphene nanoplatelets reinforced polymer nanocomposites. J Nanomater. 2013;2013:565401.

[30] Shokrieh M, Ghoreishi S, Esmkhani M, Zhao Z. Effects of graphene nanoplatelets and graphene nanosheets on fracture toughness of epoxy nanocomposites. Fatigue Fract Eng Mater Struct. 2014;37(10):1116–23.

[31] Pour ZS, Ghaemy M. Polymer grafted graphene oxide: for improved dispersion in epoxy resin and enhancement of mechanical properties of nanocomposite. Compos Sci Technol. 2016;136:145–57.

[32] Aradhana R, Mohanty S, Nayak SK. Synergistic effect of polypyrrole and reduced graphene oxide on mechanical, electrical and thermal properties of epoxy adhesives. Polymer. 2019;166:215–28.

[33] Wang X, Jin J, Song M. An investigation of the mechanism of graphene toughening epoxy. Carbon. 2013;65:324–33.

[34] Chen RS, Ruf MFHM, Shahdan D, Ahmad S. Enhanced mechanical and thermal properties of electrically conductive TPNR/GNP nanocomposites assisted with ultrasonication. PLoS One. 2019;14(9):e0222662.

[35] Yu LJ, Tarawni MA, Ahmad SH, Al-Banawi O, Batiha MA. High performance thermoplastic elastomer (TPE) nanocomposite based on graphene nanoplates (GNPs). World J Eng. 2015;12:437–42.

[36] Eriev O, Nabiev A, Karimova D, Niezov L, Mukhsinova M. Dehydrochlorination of interpolymer complexes and composites of polyanilines with poly acids. Int Polym Sci Technol. 2011;38(6):27–8.

[37] Saritha CA, Sunil KN. Polyaniline-coated short nylon fiber/ natural rubber conducting composite. Polym Plast Technol Eng. 2011;50(5):443–52.

[38] Siročić AP, Rešček A, Ščetar M, Krehula LK, Hrnjak-Murgić Z. Development of low density polyethylene nanocomposites films for packaging. Polym Bull. 2014;71(3):705–17.

[39] Liu S, Yan H, Fang Z, Wang H. Effect of graphene nanosheets on morphology, thermal stability and flame retardancy of epoxy resin. Compos Sci Technol. 2014;90:40–7.

[40] Gojny FH, Wichmann MH, Fiedler B, Bauhofer W, Schulte K. Influence of nano-modification on the mechanical and electrical properties of conventional fibre-reinforced composites. Compos Part A Appl S. 2005;36(11):1525–35.

[41] Al-Saleh MH. Electrical and mechanical properties of graphene/carbon nanotube hybrid nanocomposites. Synth Met. 2015;209:41–6.

[42] Rezvani Moghaddam A, Kamkar M, Ranjbar Z, Sundararaj U, Jannesari A, Ranjbar B. Tuning the network structure of graphene/epoxy nanocomposites by controlling edge/basal localization of functional groups. Ind Eng Chem Res. 2019;58(47):21431–40.

[43] Taherian R. Experimental and analytical model for the electrical conductivity of polymer-based nanocomposites. Compos Sci Technol. 2016;123:17–31.

[44] He L, Wang H, Zhu H, Gu Y, Li X, Mao X. Thermal properties of PEG/graphene nanoplatelets (GNPs) composite phase change materials with enhanced thermal conductivity and photothermal performance. Appl Sci. 2018;8(12):2613.

[45] Yu A, Ramesh P, Itkis ME, Bekyarova E, Haddon RC. Graphite nanoplatelet-epoxy composite thermal interface materials. J Phys Chem C. 2007;111(21):7565–9.

[46] Yu ZT, Fang X, Fan LW, Wang X, Xiao YQ, Zeng Y, et al. Increased thermal conductivity of liquid paraffin-based suspensions in the presence of carbon nano-additives of various sizes and shapes. Carbon. 2013;53:277–85.

[47] Shahdan D, Chen RS, Ahmad S. Mechanical and thermal properties of toughened polylactic acid/liquid natural rubber/polyaniline nanocomposites reinforced graphene at low loading. Sains Malays. 2020;49(9):2101–11.

[48] Tarawneh MaA, Saraireh SA, Chen RS, Ahmad SH, Al-Tarawni MAM, Al-Tweissi M, et al. Mechanical, thermal, and conductivity performances of novel thermoplastic natural rubber/graphene nanoplates/polyaniline composites. J Appl Polym Sci. 2020;137(28):48873.

[49] Yang X, Liang C, Ma T, Guo Y, Kong J, Gu J, et al. A review on thermally conductive polymeric composites: classification, measurement, model and equations, mechanism and fabrication methods. Adv Compos Hybrid Mater. 2018;1(2):207–30.

[50] Shahdan D, Chen RS, Ahmad S, Zailan FD, Mat Ali A. Assessment of mechanical performance, thermal stability and water resistance of novel conductive poly(lactic acid)/modified natural rubber blends with low loading of polyaniline. Polym Int. 2018;67(8):1070–80.

[51] Hu K, Kulkarni DD, Choi I, Tsukruk VV. Graphene-polymer nanocomposites for structural and functional applications. Prog Polym Sci. 2014;39(11):1934–72.